Calcium sensor kinase activates potassium uptake systems in gland cells of Venus flytraps

Sönke Scherzer[a,1], Jennifer Böhm[a,1], Elzbieta Krol[a], Lana Shabala[b], Ines Kreuzer[a], Christina Larisch[a], Felix Bemm[c], Khaled A. S. Al-Rasheid[d], Sergey Shabala[b], Heinz Rennenberg[e], Erwin Neher[f,2], and Rainer Hedrich[a,2]

[a]Institute for Molecular Plant Physiology and Biophysics, University of Wuerzburg, D-97082 Würzburg, Germany; [b]School of Land and Food, University of Tasmania, Hobart TAS 7001, Australia; [c]Department of Molecular Biology, Max Planck Institute for Developmental Biology, 72076 Tübingen, Germany; [d]Zoology Department, College of Science, King Saud University, Riyadh 11451, Saudi Arabia; [e]Institute of Forest Sciences, University of Freiburg, 79085 Freiburg, Germany; and [f]Department for Membrane Biophysics, Max Planck Institute for Biophysical Chemistry, D-37077 Goettingen, Germany

The Darwin plant *Dionaea muscipula* is able to grow on mineral-poor soil, because it gains essential nutrients from captured animal prey. Given that no nutrients remain in the trap when it opens after the consumption of an animal meal, we here asked the question of how *Dionaea* sequesters prey-derived potassium. We show that prey capture triggers expression of a K^+ uptake system in the Venus flytrap. In search of K^+ transporters endowed with adequate properties for this role, we screened a *Dionaea* expressed sequence tag (EST) database and identified DmKT1 and DmHAK5 as candidates. On insect and touch hormone stimulation, the number of transcripts of these transporters increased in flytraps. After cRNA injection of K^+-transporter genes into *Xenopus* oocytes, however, both putative K^+ transporters remained silent. Assuming that calcium sensor kinases are regulating *Arabidopsis* K^+ transporter 1 (AKT1), we coexpressed the putative K^+ transporters with a large set of kinases and identified the CBL9-CIPK23 pair as the major activating complex for both transporters in *Dionaea* K^+ uptake. DmKT1 was found to be a K^+-selective channel of voltage-dependent high capacity and low affinity, whereas DmHAK5 was identified as the first, to our knowledge, proton-driven, high-affinity potassium transporter with weak selectivity. When the Venus flytrap is processing its prey, the gland cell membrane potential is maintained around −120 mV, and the apoplast is acidified to pH 3. These conditions in the green stomach formed by the closed flytrap allow DmKT1 and DmHAK5 to acquire prey-derived K^+, reducing its concentration from millimolar levels down to trace levels.

Dionaea muscipula | CIPK | HAK5 | AKT | transporter

The carnivorous plant *Dionaea muscipula* actively traps small animals. To this end, it forms leaves that develop into a bilobed capture organ, with the upper surface of the modified leaf equipped with three sensory hairs per lobe. Flies, ants, and spiders, attracted by volatiles, frequently visit the traps, accidentally touching the sensory hairs, thus triggering action potentials (APs) in the trap (1). After two APs have been elicited, the trap closes within a fraction of a second (2). The prey, moving around and trying to escape, repeatedly activates the mechanosensors, which in turn, stimulate the secretion of digestive enzymes from glands lining the inner surface of the trap. The end result is that the prey in *Dionaea*'s green stomach is completely decomposed, releasing nutrients and minerals that are then available to the plant.

An uptake system for NH_4 has already been described (3). However, little is known about the uptake of potassium, which for plants, is a macronutrient required for turgor-based growth and movements (review in ref. 4). From energetic considerations, it has traditionally been proposed that high-affinity K^+ uptake in plants is an active process mediated by a K^+/H^+ symporter, whereas low-affinity, passive uptake is operated by channels (5, 6). The major K^+ uptake systems in roots, *Arabidopsis thaliana* high affinity K^+ transporter 5 (AtHAK5) and *Arabidopsis* K^+ transporter 1 (AKT1), were identified by studying *Arabidopsis thaliana* Transfer-DNA insertion lines, in which these genes are knocked out. AtHAK5 was recognized as the only high-affinity uptake system at external K^+ concentrations <10 μM, whereas both AtHAK5 and AKT1 were shown to contribute to K^+ acquisition between 10 and 200 μM. At external concentrations >500 μM, AtHAK5 is not relevant, and K^+ uptake is dominated by AKT1 (7, 8). Although activation by phosphorylation through the Ca^{2+}-dependent protein kinase complex calcineurin B-like (CBL)/CBL-interacting protein kinases (CIPK) has enabled the characterization of the transport function of AKT1, no detailed electrophysiological characterization of the high-affinity K^+ transporter has been possible so far, because HAK5 remains silent in the heterologous expression system of *Xenopus* oocytes (9). Consequently, the selectivity and regulation of HAK5 are still under debate (10).

Here, we ask the question of how the flytrap acquires prey-derived potassium ions. Our in planta experiments suggested that *Dionaea* glands operate an insect-induced, dual-affinity potassium uptake system. We, therefore, screened an expressed sequence tag (EST) collection containing RNA from glands of insect- and touch hormone-stimulated flytraps and identified orthologs of AKT1 and AtHAK5, which we name DmKT1 and DmHAK5. Activation of these proteins in *Xenopus* oocytes by coexpression with a calcium sensor kinase allowed us to provide a detailed

Significance

The Venus flytrap *Dionaea muscipula* has been in the focus of scientists since Darwin's time. Carnivorous plants, with their specialized lifestyle, including insect capture, as well as digestion and absorption of prey, developed unique tools to gain scarce nutrients. In this study, we identified the molecular nature of the uptake machinery for prey-derived potassium and the posttranslational regulation. For the first time, to our knowledge, we functionally characterize DmHAK5 here—a KUP/HAK/KT family member as activated by a CBL-CIPK kinase complex. Detailed electrophysiological characterization identified DmHAK5 as a proton-driven, high-affinity potassium transporter with a weak selectivity. Working hand-in-hand with the low-affinity, high-capacity K^+-channel DmKT1 activated by the same kinase, the transporters allow the Venus flytrap to take up prey-derived potassium.

PLANT BIOLOGY

electrophysiological characterization of the high- and low-affinity transporters DmHAK5 and DmKT1, respectively. Both proteins, when expressed in oocytes, displayed the gross features as observed in transport studies on whole *Dionaea* glands.

Results

Flytrap Ingests Prey-Derived Potassium. To study the capacity of the flytrap for intake of prey-derived potassium, we used an insect powder stock for feeding experiments (11). In a previous study, this well-defined nutrient source was successfully used to trace the intake of amino acids and ammonium (3). The insect fodder paste, which contains a K^+ concentration of 30 mM, was applied to the inner trap surface, whereupon the sensory hairs were stimulated to close the capture organ and commence secretion of digestive fluid. This protocol, designed to mimic living prey, caused the two trap lobes to form a hermetically sealed green stomach (2). By sampling the nutrient intake organs and removing any remaining fodder paste and stomach contents, we determined their time-dependent changes in potassium content. When monitoring the total trap K^+ content by inductively coupled plasma MS, we found that the level of this major plant cation started rising 4–6 h after initiating feeding and reached a steady state at 12–24 h. The higher level lasted for at least 2–3 d (Fig. 1A). The steady-state K^+ content of the fed traps was about two times that of control traps ($t = 0$ and 2 h after feeding). These results indicate that *Dionaea* has the capacity to take up and store prey-derived potassium in the capture organ. To confirm this finding and study the potassium intake at a higher resolution, we complemented the insect paste with the K^+-tracer Rb^+ at concentrations of 30 (Fig. 1A), 3, and 0.3 mM (Fig. S1). Apart from starting from a zero level, the Rb^+ concentration of traps showed the same kinetics of increase as that

Fig. 1. K^+ uptake in *Dionaea* traps. (A) Traps were fed with standardized insect powder, and both time-dependent K^+ and Rb^+ uptakes were analyzed. After 12 h of digestion, both the K^+ and Rb^+ concentrations in fed traps doubled compared with unfed traps (time = 0). (B) Using MIFE experiments with unstimulated (black) and COR-treated (red) *Dionaea* traps, K^+ influxes were measured in response to the indicated external K^+ concentrations. High-affinity K^+ influx was obtained in COR-treated traps only. After the normalization of K^+ fluxes to 1 at 1 mM K^+, data points could be best fitted with a Michaelis–Menten function (solid line), revealing a K_m value of 0.06 ± 0.01 mM ($n \geq 7$; mean $\pm$ SD). (C) K^+ uptake triggered membrane depolarizations in *Dionaea* glands on application of 0.6 or 2 mM external K^+. (D) High- and low-affinity response curves of gland cell membrane depolarizations (red and black, respectively) and normalized currents (blue) of DmKT1/DmHAK5/CBL9/CIPK23-coexpressing oocytes at various external K^+ concentrations. Curves in the two concentration ranges were independently fitted with Michaelis–Menten equations to obtain the indicated half-maximal depolarizations (EC_{50} values; mean membrane depolarization $\pm$ SD; $3 \leq n \leq 8$).

determined for K^+. Rubidium uptake was already visible at a food stock concentration of 0.3 mM and increased with increasing Rb^+ concentration (Fig. S1).

Gland K^+ Uptake Displays Both Low- and High-Affinity Transport Components. To study the K^+ uptake, we monitored the K^+ fluxes into the gland-covered inner trap surface using the vibrating ion-selective electrode technique microelectrode ion flux measuring (MIFE) (12, 13). Single-trap lobes were fixed to a chamber, and ion-selective microelectrodes were placed close to the trap surface, which is densely packed with about 37,000 glands per trap (2), monitoring K^+ fluxes under different external K^+ concentrations. Unstimulated traps did not take up any external K^+ in the high-affinity range. In contrast, when traps were pretreated with the touch hormone mimic coronatine [COR; a substitute for insect stimulation (2)], macroscopic inward K^+ fluxes were detected (Fig. 1B and Fig. S2A). When we increased K^+ concentration stepwise from 0.01 to 1 mM with media buffered to pH 4, electrodes registered inward fluxes of up to 200 nmol m^{-2} s^{-1} in COR-stimulated traps. Fluxes tended to saturate, reaching a steady state at ~500 μM external K^+ (Fig. 1B and Fig. S2A). By fitting a Michaelis–Menten equation to the K^+ dose–response curve in this low-concentration range, a half-saturation concentration of about 60 μM was calculated (Fig. 1B). This apparent K_m value is in line with a high-affinity potassium uptake system (ref. 14 and references therein). Such a system requires energy from either an electrical and/or a chemical gradient. Uphill carrier transport of many solutes is coupled to the downhill movement of protons (15–17). When we shifted the pH from 4 to 8, COR-induced potassium fluxes were completely suppressed, indicating that high-affinity trap K^+ uptake is driven by a proton gradient (Fig. S2B).

Increasing the external K^+ concentration to values much higher than the K_m of the high-affinity transport further increased the fluxes. At 10 mM K^+, inward fluxes as high as or even above 1,000 nmol m^{-2} s^{-1} (10 times the maximum value of the high-affinity transport) were detected. These high-capacity fluxes point to the presence of a low-affinity transport system in addition to the low-capacity, high-affinity component (Fig. S2C). The fact that even unstimulated traps respond to high external K^+ concentrations points to a basal expression of the low-affinity component compared with the high-affinity uptake system.

Extracellular electrodes provide a noninvasive assay of trap K^+ fluxes, but they do not report the membrane potential of the cells engaged with K^+ transport, a quantity required for thermodynamic considerations. Influx of potassium ions and protons into gland cells is expected to depolarize their membrane potential. To monitor the predicted membrane response of gland cells, we inserted sharp impalement electrodes into cells of layer 1 or 2 of the dome-shaped glands. At pH 4 and 0.1 mM external K^+, we recorded a resting potential around −140 mV for both insect and COR-stimulated gland cells (cf. 3). The addition of 2 mM K^+ depolarized the membrane potential of stimulated glands (Fig. 1C, red line). Given a gland cell cytoplasmic potassium load of 100 mM and a green stomach concentration above 1 mM K^+, an electrical force of $\leq$−120 mV would theoretically suffice to drive K^+ influx through an acid pH-activated potassium channel (18). At an external potassium level lower than 1 mM, however, the gland cell membrane potential would not be able to energize transport against a potassium concentration gradient greater than 100-fold if it was mediated by a channel-like mechanism. However, the application of 0.6 mM K^+ at pH 4 still resulted in a potassium-dependent depolarization in the same range. This finding points toward a high-affinity K^+ transport mechanism, a system that is not only energized by the membrane potential gradient (Fig. 1C, black line). By plotting the depolarization against the applied K^+ concentration, a biphasic character becomes evident (Fig. 1D, red). The high-affinity component in
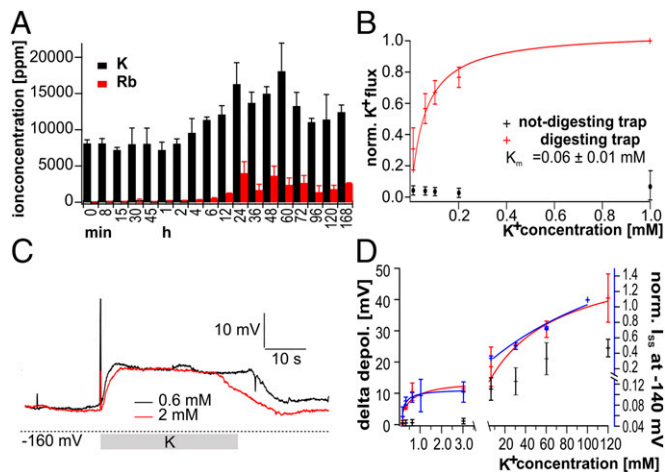
K$^+$ uptake reaches its half-maximum activity at 0.48 ± 0.38 mM, whereas the low-affinity transport does so at 65.48 ± 33.7 mM external K$^+$ (Fig. 1D). Performing the same experiment with unstimulated gland cells (Fig. 1D, black), we find almost no depolarization in the high-affinity range. When we further increase the K$^+$ concentration to the low-affinity range, a distinct depolarization in unstimulated gland cells becomes obvious. This investigation points to a different expressional regulation of high- and low-affinity transporters during digestion.

Thus, our impalement electrode recordings together with the MIFE measurements indicate that gland cells of insect and COR-stimulated traps possess both a high-affinity, pH-dependent K$^+$/H$^+$ symport and a low-affinity, high-capacity K$^+$ transport system.

Stimulated Glands Express AKT-Like Potassium Channel and HAK-Type K$^+$-Transporter Genes.

To elucidate the genes encoding *Dionaea*'s gland potassium uptake system, we searched an EST database (cf. 3, 19, and 20), identifying the AKT1-like, *Shaker*-type potassium channel ortholog DmKT1 and the HAK-type transporter DmHAK5 as potential candidates. Both proteins were found to be expressed and up-regulated in digesting glands of the Venus flytrap. Detailed information is in SI Text, section 1 and Fig. S3 *A and B*.

Dionaea's K$^+$ Transport Requires Activation by a Calcium Signaling Kinase.

Xenopus laevis oocytes are widely used to express genes from different taxa. The function of *Arabidopsis* AKT1 when expressed in this system depends on phosphorylation by a calcium sensor kinase of the CBL/CIPK type (21, 22). We also found orthologs of CIPK23 and CBL9 expressed in *Dionaea*. In contrast to AKT1 (21, 22), however, HAK5 transporters do not seem to be functionally expressed in this animal expression system, which is plant background-free. Consequently, no detailed electrophysiological characterization of HAK transporters has been possible (9, 23). Given that, in *Arabidopsis*, the AKT1 potassium channel function depends on a CBL/CIPK pair, we reasoned that, in *Dionaea*, AKT1 and probably, HAK5 orthologs could also depend on a similar calcium sensor kinase complex. Indeed, expression of DmKT1-mediated macroscopic inward K$^+$ currents is only in the presence of the *Arabidopsis* CBL9/CIPK23 pair, which also activates its *Arabidopsis* ortholog AKT1 (Fig. S4 *A–C*) (21, 22).

Regarding HAK-type transporters, we first performed an experiment similar to that in the work by Kim et al. (9), which studied a high-affinity KUP/HAK/KT family member. Just like in the work by Kim et al. (9), we were not able to observe macroscopic K$^+$ currents in *Xenopus* oocytes expressing DmHAK5 cRNA alone (Fig. 2A). However, we then expressed DmHAK5 together with various CBL/CIPK combinations and found substantial inward currents (Fig. 2) when using the CBL9/CIPK23 pair and K$^+$-containing buffers at a pH of 4. The requirement of pH 4 is not surprising given that, on prey processing, *Dionaea*'s stomach acidifies. The notion that both DmHAK5 and DmKT1 may interact with the CIPK23 was supported by bimolecular fluorescence complementation-based protein–protein interaction assays (Fig. S4 *D–G*) (cf. 24). Thus, the same calcium sensor kinase, CIPK23, regulates the transport function of both DmKT1 and DmHAK5. We conclude that the calcium-dependent kinase acts as a key regulator for both the low- and high-affinity potassium uptakes in *Dionaea* glands.

DmKT1 Is a K$^+$-Selective Channel with Voltage- and pH-Dependent Gating.

As with other members of the *Shaker*-like K$^+$-channel family, DmKT1 is classified as a voltage-dependent inward-rectifying K$^+$ channel. When the AKT1 ortholog from *Dionaea* was coexpressed with CBL9/CIPK23, a typical hyperpolarization-activated, inward-rectifying K$^+$-channel activation was observed under 100 mM external K$^+$ (Fig. S4 *A–C*). Animals contain potassium and sodium at about similar concentrations (25, 26).
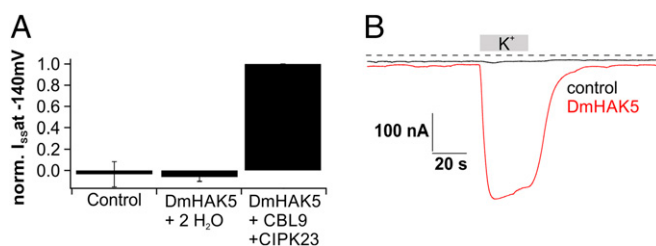

Fig. 2. Transport activation of DmHAK5. (*A*) Normalized current response recorded at -140 mV of *Xenopus* oocytes injected with H$_2$O, cRNA of DmHAK5, or cRNA of DmHAK5 supplemented with CBL9/CIPK23. Macroscopic potassium currents were only detectable in DmHAK5/CBL9/CIPK23-coexpressing oocytes in solutions containing 2 mM potassium ($n \geq 6$; mean $\pm$ SD). (*B*) Typical whole-oocyte currents recorded at -60 mV of an H$_2$O-injected (black) and a DmHAK5/CBL9/CIPK23-expressing (red) *Xenopus* oocyte. Addition of 2 mM K$^+$ resulted in macroscopic inward currents of $\sim$400 nA only with DmHAK5-expressing oocytes. The dotted line represents zero current.

When prey are decomposed in *Dionaea*'s green stomach, the K$^+$ uptake system is exposed to both monovalent cations. We therefore investigated the cation selectivity of the flytrap AKT1 ortholog. Oocytes were incubated with solutions containing Li$^+$, Na$^+$, K$^+$, Rb$^+$, Cs$^+$, NH$_4^+$, or *N*-methyl-D-glucamine (NMDG$^+$) at 100 mM concentration. However, DmKT1-mediated cation inward currents were observed in potassium-based buffers only (Fig. 3A). On a 10-fold change in bath K$^+$ concentration from 10 to 100 mM, a near-Nernstian shift in reversal potential (53.80 ± 1.06 mV; $n = 6 \pm$ SD) was observed, indicating that DmKT1 is a K$^+$-selective channel. With the acidification during prey digestion, this K$^+$ channel is additionally confronted with a high external H$^+$ concentration. When oocytes were superfused with 100 mM KCl, a distinct increase in K$^+$ inward current was observed when the pH was lowered stepwise from 6 to 3 (Fig. 3 *B and C*). Interestingly, any shift in reversal potential in response to this change in proton concentration by three orders of magnitude was insignificant from zero (-0.43 ± 3.06 mV; $n = 6 \pm$ SD; $P > 0.5$ by one-way ANOVA). This result documents that H$^+$ is not transported by the channel. A Boltzmann analysis of DmKT1 channel activity at an external pH of 6 revealed a voltage dependence with a half-maximal activation potential ($V_{1/2}$) of -129.64 ± 3.06 mV. Increasing the external H$^+$ concentration shifts this potential to more positive values, reaching a $V_{1/2}$ of -78.29 ± 2.35 mV at pH 3 (Fig. 3D). These findings are in line with an acid-induced shift in the open probability (P_O) of the channel (cf. 27).

DmHAK5 Is an H$^+$-Driven K$^+$ Transporter.

The fact that even rubidium, which is commonly used as a potassium tracer, does not permeate DmKT1 (Fig. 3A) raises questions about the transport of rubidium in experiments with insect powder feeding (Fig. 1A and Fig. S1). We therefore superfused oocytes expressing DmHAK5 and CBL9/CIPK23 with a sorbitol-based solution of pH 4 supplemented with 2 mM Li$^+$, Na$^+$, K$^+$, Rb$^+$, Cs$^+$, NH$_4^+$, or NMDG$^+$ (Fig. 4 *A and B*). In the presence of potassium and rubidium ions, DmHAK5-mediated inward currents were of similar amplitudes, whereas the currents with caesium and ammonium as charge carriers were reduced by 65–50%. Lithium, sodium, and NMDG ions at 2 mM concentration did not evoke DmHAK5-mediated currents (Fig. 4 *A and B*).

In the green stomach, the selective K$^+$ uptake will decrease the external K$^+$ concentration to very low levels, but Na$^+$ might remain high. Consequently, we asked whether DmHAK5 would still be impermeable to Na$^+$ under such conditions and monitored the currents of DmHAK5-expressing oocytes at a Na$^+$ concentration 50 times higher compared with the K$^+$ concentration of 2 mM. Currents were the same as those recorded during replacement of Na$^+$ by sorbitol (Fig. 4C). Also, in the
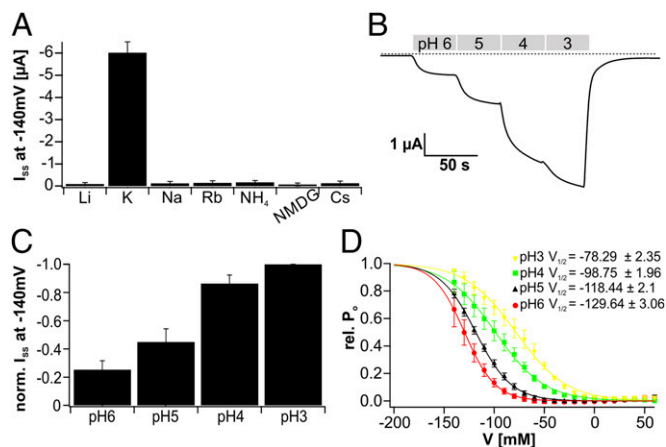
PLANT BIOLOGY

Fig. 3. Selectivity and pH dependency of DmKT1. (*A*) Currents recorded at −140 mV of DmKT1/CBL9/CIPK23-expressing oocytes in the presence of bath solutions containing various monovalent cations (each 100 mM). Large cat-ion influx was only obtained with potassium in the external bath solution (*n* = 4; mean ± SD). (*B*) Inward K⁺ currents elicited by a DmKT1/CBL9/CIPK23-expressing *Xenopus* oocyte markedly increased on acidification of the ex-ternal solution (V_m = −100 mV). Exchanging 100 mM external Li⁺ for 100 mM K⁺ at pH 6 resulted in potassium influx, which was enhanced by increasing the external H⁺ concentration. The dotted line represents zero currents. (*C*) Normalized currents of DmKT1/CBL9/CIPK23-expressing *Xenopus* oocytes at −140 mV. Stepwise acidification from pH 6 to 3 increased the potassium currents through DmKT1 (*n* = 6; mean ± SD). (*D*) The relative open proba-bility (rel. P_O) of DmKT1-expressing oocytes at the indicated H⁺ concentra-tions was plotted against the applied test voltage. Note the prominent positive shift of the half-maximal activation potential ($V_{1/2}$) with increasing acidification. The data points were fitted with a Boltzmann function (solid lines; *n* = 6; mean ± SD).

absence of K⁺, currents were small and similar in amplitude, regardless of whether 100 mM Na⁺ or sorbitol was present. This finding shows that, even under conditions of high sodium back-ground, which might be found in the green stomach, DmHAK5 remains Na⁺-impermeable and that transporter activity is un-affected by Na⁺.

As mentioned above, gland acid secretion can lower the pH in the green stomach to a value of 3 or even lower (2), and MIFE experiments displayed a pH dependency of K⁺ transport. To study these effects in more detail, we exposed oocytes expressing the activated DmHAK5 to a saturating K⁺ concentration, while varying the H⁺ concentration. Compared with control oocytes, an increasing K⁺ current at pH ≤ 5 was observed (Fig. 4*D*). This finding is well in line with the in planta recordings and supports the hypothesis of an H⁺-driven, high-affinity K⁺ symport.

DmKT1 Has High Capacity and Low Affinity, Whereas DmHAK5 Has Low Capacity and High Affinity. To explore whether both *Dio-naea* gland K⁺ uptake systems act complementary to each other, we analyzed their affinity to their major substrates. With oocytes expressing the calcium sensor kinase-activated DmKT1 or DmHAK5, we stepwise increased the external potassium con-centration in buffers of pH 4. In the presence of 5 mM external K⁺ and at −140 mV, DmKT1-expressing oocytes supported an inward current of 0.15 ± 0.06 μA, which increased up to 6.42 ± 0.32 μA when the K⁺ concentration was raised to a maximum of 100 mM (Fig. S5*A*). A plot of current against [K⁺] could be fitted with a Michaelis–Menten function, with a K_m value of 108.29 ± 7.34 mM (Fig. 5*A*).

Likewise, a rising inward current was observed when super-fusing DmHAK5-expressing oocytes with increasing K⁺ concen-trations under similar conditions. However, the dose–response curve in this case could be fitted with a Michaelis–Menten

equation with a K_m value of 127.38 ± 2.77 μM (Fig. 5*B*) (850 times lower than that of DmKT1). These features and the temperature dependence (*SI Text*, section 2 and Fig. S6 *A and B*) of DmHAK5 are well in line with a low-capacity, high-affinity, proton-driven K⁺ transporter, which was observed by MIFE and impalement ob-servations of whole *Dionaea* glands. When we coexpressed DmKT1 together with DmHAK5 in oocytes, we observed a bi-phasic K⁺ uptake (Fig. 1*D*, blue). This combined behavior of the two transporters is reminiscent of the gland K⁺ response (Fig. 1*D*, red).

Low Extracellular Potassium Leads to Decreased Conductance of DmKT1. To gain additional insights into the molecular basis of channel activity at different external K⁺ concentrations, we per-formed a quantitative comparison of DmKT1 activation curves by analyzing the channel's cord conductance G_K (cf. 28) (*Methods*). This quantity was shown to be a good estimation for the voltage-dependent channel conductance in *Arabidopsis* AKT1 and KAT1. Plots of G_K vs. voltage, obtained at various K⁺ concentrations, were well-described by Boltzmann functions (Fig. 5*C*). They revealed that G_K of DmKT1 decreased on lowering the external K⁺ concentration. Decreasing the external K⁺ concentrations from 100 to 5 mM, the cord conductance decreased by nearly 82% (Fig. 5*C*). The deduced maximal cord conductance (G_{K-max}), which was derived from the Boltzmann fittings, was plotted against the corresponding K⁺ concentrations (Fig. 5*D*). The resulting saturation curve could be best described by a Michaelis–Menten equation and yielded a half-maximal value ($K_{0.5}$) of 34 mM ex-ternal potassium. How can this behavior be explained? Using biophysical approaches, it had been shown that the *Arabidopsis* potassium channel KAT1 is K⁺-sensitive in the low millimolar range ($K_{0.5}$ of 1.4 mM), whereas *Arabidopsis* AKT1 is K⁺-sensitive
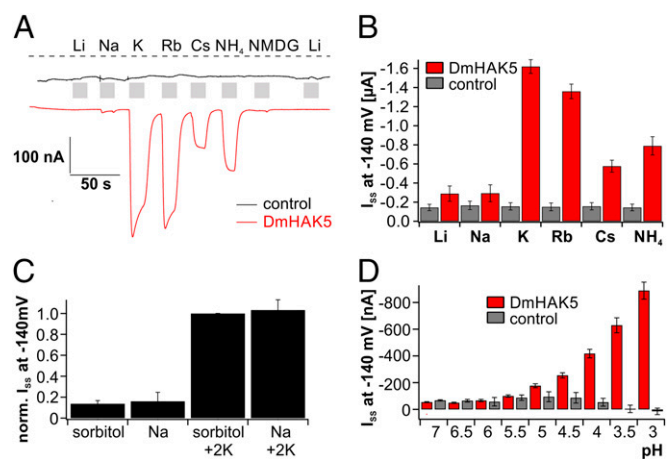

Fig. 4. Selectivity and pH dependency of DmHAK5. *Xenopus* oocytes were either injected with H_2O (control) or cRNA of DmHAK5/CBL9/CIPK23 (DmHAK5). (*A*) Representative current recordings at −60 mV of a control (black) and a DmHAK5-expressing (red) *Xenopus* oocyte in response to 2 mM Li⁺, Na⁺, K⁺, Rb⁺, Cs⁺, NH₄⁺, or NMDG⁺ (as indicated using sorbitol-based solutions). Both K⁺ and Rb⁺ resulted in macroscopic inward currents with DmHAK5-expressing oocytes. Application of NH₄⁺ and Cs⁺ induced weaker DmHAK5-mediated inward currents. The dotted line represents zero current. (*B*) Average results from experiments as shown in *A*, except that the holding potential was −140 mV (*n* = 7; mean ± SD). (*C*) Normalized steady-state currents of *Xenopus* oocytes injected with DmHAK5 were recorded at −140 mV in response to sorbitol- or Na⁺-based solution (200 mOsm/kg). Addition of 2 mM K⁺ resulted in identical K⁺ influx irrespective from the presence or absence of sodium in the bath solution (*n* = 7; mean ± SD). (*D*) I_{ss} recorded at −140 mV with oocytes injected with either H_2O (gray bars) or DmHAK5 (red bars) in the presence of 100 mM K⁺ at different pH values (as indicated; *n* = 5; mean ± SD). Compared with control oocytes, K⁺ currents increased at pH values ≤5.
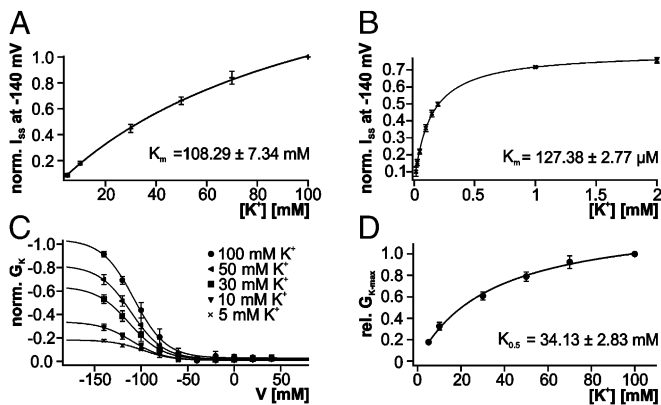
Fig. 5. Biophysical analysis of DmKT1- and DmHAK5-mediated K^+ currents at varying extracellular K^+ concentrations. (*A*) Dose–response curve of DmKT1/CBL9/CIPK23-expressing *Xenopus* oocytes at −140 mV. The ionic strength of the solutions with varying K^+ concentrations was adjusted to 100 mM with Li^+. The saturation curve could be best fitted with a Michaelis–Menten equation (solid line), documenting a K_m value of 108.29 ± 7.34 mM for DmKT1 ($n = 5$; mean ± SD). (*B*) Dose–response curve of DmHAK5/CBL9/CIPK23-expressing *Xenopus* oocytes clamped to a membrane potential of −140 mV. The Michaelis–Menten fit revealed a K_m value of 127.38 ± 2.77 μM for DmHAK5 ($n = 6$; mean ± SD). (*C*) G_K/V relationship of DmKT1-expressing oocytes in a K^+ concentration range from 100 to 5 mM. Data points were normalized to G_K at −140 mV in 100 mM K^+ and fitted with a Boltzmann function. Decreasing the potassium concentration leads to a reduction in the cord conductance but not a change of the voltage dependence of the relative open probability (see also Fig. S5*B*) ($n = 5$; mean ± SD). (*D*) The relative maximal cord conductance was calculated with the equation: $G_{K-max} = G_{K-max}(X$ mM)/G_{K-max} (100 mM). Data points were plotted against the applied K^+ concentration and fitted with a Michaelis–Menten equation. Note that G_{K-max} increased with increasing potassium concentrations with a half-maximal activity ($K_{0.5}$) of 34 mM ($n = 5 ±$ SD).

at higher concentrations ($K_{0.5}$ of 16.2 mM) (28, 29). In both studies, the inhibition of KAT1 and AKT1 has been associated with a pore collapse at low external K^+ concentrations. We found that the open probability of DmKT1 is only weakly affected by K^+ concentration changes (*SI Text, section 3* and Fig. S5*B*). Therefore, the major G_K reduction of DmKT1 is also most likely caused by the reduction of the number of activatable channels at moderate external potassium concentrations. The higher sensitivity to low external K^+ of DmKT1 compared with *Arabidopsis* K^+ channels very likely represents an adaption to the needs within the *Dionaea* digestive organ. By inactivating DmKT1 under conditions of outward-directed K^+ driving forces, *Dionaea* prevents K^+ leakage from the gland cells.

Discussion

The carnivorous Darwin plant *Dionaea* is equipped with a unique sensory system and information management through APs to capture prey and then, digest its nutrients (30). Because *Dionaea* is a nonmodel, nontransformable plant, we used a recently established gain-of-gene function approach (3, 31) and revealed the trap transporters engaged in potassium uptake. We document that transcription of a *Dionaea* HAK5-type transporter in glands is induced by prey capture and the presence of jasmonate-type touch hormones. In addition to DmHAK5, we found that a *Shaker*-type DmKT1 channel is also expressed in *Dionaea* glands. We cloned and expressed both DmHAK5 and DmKT1 in the *Xenopus* oocytes system, which is free of any plant background. Nevertheless, in this heterologous system, both transporters have the same fingerprint as they do in their native flytrap.

In these specialized organs, like in roots of the model plant *A. thaliana*, the HAK5 K^+ transporter and AKT1 K^+ channel represent the two major complementary systems for K^+ uptake

(8, 14). Interestingly, we found that the DmHAK5 K^+/H^+ cotransporter is posttranslationally activated by the same CBL/CIPK complex as the AKT1-type *Shaker* channel (21). The HAK-type transporter is apparently the only system capable of operating at micromolar K^+ concentrations (14). The first high-affinity K^+-transporter HAK1 was cloned from *Schwanniomyces occidentalis*, an ascomycete yeast that is able to grow in a nutrient-poor environment and can accumulate potassium when the available external concentrations are in the low sub-micromolar range (32). *Dionaea* faces a very similar situation, and it is able to obtain K^+ from the captured animal nutrient source, even when concentrations are at trace levels.

During digestion of *Dionaea*'s prey, acidification in the external stomach shifts the open probability of DmKT1 to more positive values, thus allowing this channel to activate. Given that the cytoplasm of the gland cells contains 100 mM potassium and that the membrane potential of a digesting *Dionaea* gland is about −120 mV, this K^+-selective channel can acquire external K^+ passively down to a value of 1 mM. Below this concentration, the K^+ flux would be reversed if the channels would remain open, the result of the outwardly directed electrochemical driving force. Nonetheless, such K^+ leakage is prevented by a reduction of channel activity under low external K^+.

In this study, we were able to activate an HAK-type transporter for the first time, to our knowledge, in *Xenopus* oocytes. We found that DmHAK5 is of low selectivity, transporting $K^+ = Rb^+ \geq NH_4^+ \geq Cs^+$. Interestingly, Na^+ is neither a substrate nor a modulator of the HAK5-type transporter in *Dionaea*. The influence of this cation without having the transporter functionally expressed in oocytes was still unclear and a matter of debate (33–38).

By reporting a K_m of 127 μM, we clearly classify DmHAK5 as a high-affinity transporter that is active at K^+ concentrations too low for K^+ uptake by DmKT1. During the absorption of a prey's mineral deposits, K^+ concentration drops to 10 μM, which leads to the question of how DmHAK5 energizes an uphill transport against a 10,000-fold concentration gradient under the assumption of a 100 mM cytosolic K^+. To overcome such a high gradient, a passive K^+ channel would only generate an influx at a membrane potential (electrical potential) more negative than −240 mV. However, the membrane potential of gland cells, even during prey digestion and nutrient uptake, is maintained around −120 mV (cf. this study and 3). To overcome this problem, DmHAK5, acting as a K^+/H^+ symporter, uses the chemical potential of the proton in addition to the electrical potential. Assuming a cytosolic pH of the gland cells of 7 and a pH of 3 or lower for the prey-digesting acidic fluid in the green stomach, the proton-motive force would add the equivalent of an additional −240 mV to the membrane potential. From thermodynamic considerations, the combined force would allow the flytrap to accumulate K^+ more than 100,000-fold. Other than this thermodynamic consideration and the pH dependence of DmHAK5-mediated transport, final proof for K^+/H^+ coupling and stoichiometry requires measurements on the K^+- and H^+-dependent shift in reversal potential.

Thus, both proteins are activated by the same calcium-dependent kinase and work together to provide an orchestrated acquisition of potassium. With the high capacity of DmKT1 and the high affinity of DmHAK5, this K^+ uptake module within the green stomach is able to sequester the prey-derived potassium rapidly when the potassium concentration is relatively high as well as reduce it to very low remnant levels.

Methods

Cloning of DmKT1 and DmHAK5. In brief, we used an available EST database from *D. muscipula* (19) and identified coding sequences related to potassium transporter homologs. Putative transporter genes were cloned into oocyte

expression vectors (39), and cRNAs were injected into *Xenopus* oocytes for functional analysis. Detailed information is in *SI Methods*.

Plant Material and Tissue Sampling. *D. muscipula* plants were purchased from CRESCO Carnivora and grown in plastic pots at 22 °C in a 16-h light/8-h dark photoperiod. The material for the expression analyses was treated as described elsewhere (3).

Feeding Experiments. For rubidium and potassium uptake measurements, traps were fed with 20 mg insect powder and dispensed in 100 μL water or RbCl solution to obtain the desired Rb$^+$ concentration. Insect powder was produced from adult moths of *Vanessa cardui* (Lep.: Nymphalidae), which had K$^+$ content that was ∼30 mM; 24 h after feeding, traps were harvested, the remaining insect material was removed, and the plant tissue was completely dried. Subsequently, the ground plant powder was digested with HNO$_3$ in a pressure ashing device (Seif). Samples diluted with H$_2$O were analyzed by inductively coupled plasma optical emission spectroscopy (JY 70 Plus; Devision d'Instruments S.A.).

Expression Analyses. RNA was separately isolated from each sample and transcribed into cDNA using M-MLV Reverse Transcriptase (Promega). Quantifications of the actin transcript DmACT (GenBank accession no. KC285589) and DmHAK5 transcript were performed by real-time PCR as described elsewhere (40). DmHAK5 transcripts were normalized to 10,000 molecules DmACT.

In a second approach, transcript levels of DmHAK5 and DmKT1 after stimulation with insects and COR were measured with RNA sequencing (RNA-seq). RNA-Seq by expectation-maximization (RSEM) (10.1186/1471-2105-12-323) was used to quantify expression levels based on an assembled transcriptome. DNA-sequencing (DNA-Seq) (10.1186/gb-2010-11-10-r106)

was used to normalize between samples and experiments for the final visualization.

Noninvasive Ion Flux Measurements. Net K$^+$ fluxes were measured using non-invasive MIFE technique (University of Tasmania). The theory of noninvasive MIFE measurements and all specific details of microelectrode fabrication and calibration are described in *SI Methods* and prior publications (12, 13, 41).

Intracellular Measurements. Before measurements, the lobe of a cut trap was glued to the bottom of a chamber and left for recovery (30 min) in a standard solution containing 0.1 mM KCl, 10 mM CaCl$_2$, and 150 mM MES adjusted with Tris to pH 4. Osmolarity was kept at 240 mOsm/kg with D-sorbitol when needed. KCl supplementing standard solution was at concentrations of 0.15, 0.3, 0.6, 3, 6, 30, 60, and 120 mM. Detailed information is in *SI Methods*.

Oocyte Recordings. Oocyte preparation and cRNA generation and injection have been described elsewhere (3, 24, 28, 42). In two-electrode voltage-clamp studies, oocytes after 2 or 3 d of expression were perfused with ND 96-based solutions. Detailed information regarding solutions, pulse protocols, and data analysis is in *SI Methods*.

1. Kreuzwieser J, et al. (2014) The Venus flytrap attracts insects by the release of volatile organic compounds. *J Exp Bot* 65(2):755–766.
2. Escalante-Pérez M, et al. (2011) A special pair of phytohormones controls excitability, slow closure, and external stomach formation in the Venus flytrap. *Proc Natl Acad Sci USA* 108(37):15492–15497.
3. Scherzer S, et al. (2013) The Dionaea muscipula ammonium channel DmAMT1 provides NH$_4^+$ uptake associated with Venus flytrap's prey digestion. *Curr Biol* 23(17):1649–1657.
4. Hedrich R (2012) Ion channels in plants. *Physiol Rev* 92(4):1777–1811.
5. Maathuis FJM, Sanders D (1996) Mechanisms of potassium absorption by higher plant roots. *Physiol Plant* 96(1):158–168.
6. Rodríguez-Navarro A (2000) Potassium transport in fungi and plants. *Biochim Biophys Acta* 1469(1):1–30.
7. Chérel I, Lefoulon C, Boeglin M, Sentenac H (2014) Molecular mechanisms involved in plant adaptation to low K(+) availability. *J Exp Bot* 65(3):833–848.
8. Alemán F, Nieves-Cordones M, Martínez V, Rubio F (2011) Root K(+) acquisition in plants: The Arabidopsis thaliana model. *Plant Cell Physiol* 52(9):1603–1612.
9. Kim EJ, Kwak JM, Uozumi N, Schroeder JI (1998) AtKUP1: An Arabidopsis gene encoding high-affinity potassium transport activity. *Plant Cell* 10(1):51–62.
10. Kronzucker HJ, Britto DT (2011) Sodium transport in plants: A critical review. *New Phytol* 189(1):54–81.
11. Kruse J, et al. (2014) Strategy of nitrogen acquisition and utilization by carnivorous Dionaea muscipula. *Oecologia* 174(3):839–851.
12. Shabala SN, Newman IA, Morris J (1997) Oscillations in H$^+$ and Ca^{2+} ion fluxes around the elongation region of corn roots and effects of external pH. *Plant Physiol* 113(1):111–118.
13. Shabala S, et al. (2006) Extracellular Ca^{2+} ameliorates NaCl-induced K$^+$ loss from Arabidopsis root and leaf cells by controlling plasma membrane K+ -permeable channels. *Plant Physiol* 141(4):1653–1665.
14. Rubio F, et al. (2014) A low K$^+$ signal is required for functional high-affinity K$^+$ uptake through HAK5 transporters. *Physiol Plant* 152(3):558–570.
15. Fischer WN, et al. (2002) Low and high affinity amino acid H$^+$-cotransporters for cellular import of neutral and charged amino acids. *Plant J* 29(6):717–731.
16. Schumacher K (2014) pH in the plant endomembrane system-an import and export business. *Curr Opin Plant Biol* 22:71–76.
17. Carpaneto A, et al. (2005) Phloem-localized, proton-coupled sucrose carrier ZmSUT1 mediates sucrose efflux under the control of the sucrose gradient and the proton motive force. *J Biol Chem* 280(22):21437–21443.
18. Brüggemann L, et al. (1999) Channel-mediated high-affinity K$^+$ uptake into guard cells from Arabidopsis. *Proc Natl Acad Sci USA* 96(6):3298–3302.
19. Schulze WX, et al. (2012) The protein composition of the digestive fluid from the venus flytrap sheds light on prey digestion mechanisms. *Mol Cell Proteomics* 11(11):1306–1319.
20. Paszota P, et al. (2014) Secreted major Venus flytrap chitinase enables digestion of Arthropod prey. *Biochim Biophys Acta* 1844(2):374–383.
21. Xu J, et al. (2006) A protein kinase, interacting with two calcineurin B-like proteins, regulates K$^+$ transporter AKT1 in Arabidopsis. *Cell* 125(7):1347–1360.
22. Li L, Kim BG, Cheong YH, Pandey GK, Luan S (2006) A Ca^{2+} signaling pathway regulates a K$^+$ channel for low-K response in Arabidopsis. *Proc Natl Acad Sci USA* 103(33):12625–12630.
23. Hong JP, et al. (2013) Identification and characterization of transcription factors regulating Arabidopsis HAK5. *Plant Cell Physiol* 54(9):1478–1490.
24. Geiger D, et al. (2010) Guard cell anion channel SLAC1 is regulated by CDPK protein kinases with distinct Ca^{2+} affinities. *Proc Natl Acad Sci USA* 107(17):8023–8028.
25. Finke MD (2013) Complete nutrient content of four species of feeder insects. *Zoo Biol* 32(1):27–36.
26. Ajai AI, B M, Jacob JO, Audu UA (2013) Determination of some essential minerals in selected edible insects. *African Journal of Pure and Applied Chemistry* 7(5):194–197.
27. Hoth S, et al. (1997) Molecular basis of plant-specific acid activation of K$^+$ uptake channels. *Proc Natl Acad Sci USA* 94(9):4806–4810.
28. Geiger D, et al. (2009) Heteromeric AtKC1middle dotAKT1 channels in Arabidopsis roots facilitate growth under K$^+$-limiting conditions. *J Biol Chem* 284(32):21288–21295.
29. Hertel B, et al. (2005) KAT1 inactivates at sub-millimolar concentrations of external potassium. *J Exp Bot* 56(422):3103–3110.
30. Burdon-Sanderson J (1873) Note on the electrical phenomena which accompany stimulation of the leaf of Dionaea muscipula. *Proc R Soc Lond B Biol Sci* 21(139-147):495–496.
31. Brownlee C (2013) Carnivorous plants: Trapping, digesting and absorbing all in one. *Curr Biol* 23(17):R714–R716.
32. Bañuelos MA, Klein RD, Alexander-Bowman SJ, Rodríguez-Navarro A (1995) A potassium transporter of the yeast Schwanniomyces occidentalis homologous to the Kup system of Escherichia coli has a high concentrative capacity. *EMBO J* 14(13):3021–3027.
33. Rubio F, Alemán F, Nieves-Cordones M, Martínez V (2010) Studies on Arabidopsis athak5, atakt1 double mutants disclose the range of concentrations at which AtHAK5, AtAKT1 and unknown systems mediate K uptake. *Physiol Plant* 139(2):220–228.
34. Qi Z, et al. (2008) The high affinity K$^+$ transporter AtHAK5 plays a physiological role in planta at very low K$^+$ concentrations and provides a caesium uptake pathway in Arabidopsis. *J Exp Bot* 59(3):595–607.
35. Spalding EP, et al. (1999) Potassium uptake supporting plant growth in the absence of AKT1 channel activity: Inhibition by ammonium and stimulation by sodium. *J Gen Physiol* 113(6):909–918.
36. Bertl A, Reid JD, Sentenac H, Slayman CL (1997) Functional comparison of plant inward-rectifier channels expressed in yeast. *J Exp Bot* 48(Spec No):405–413.
37. Qi Z, Spalding EP (2004) Protection of plasma membrane K$^+$ transport by the salt overly sensitive1 Na$^+$-H$^+$ antiporter during salinity stress. *Plant Physiol* 136(1):2548–2555.
38. Aleman F, Nieves-Cordones M, Martinez V, Rubio F (2009) Differential regulation of the HAK5 genes encoding the high-affinity K$^+$ transporters of Thellungiella halophila and Arabidopsis thaliana. *Environ Exp Bot* 65(2-3):263–269.
39. Nour-Eldin HH, Hansen BG, Norholm MH, Jensen JK, Halkier BA (2006) Advancing uracil-excision based cloning towards an ideal technique for cloning PCR fragments. *Nucleic Acids Res* 34(18):e122.
40. Escalante-Pérez M, et al. (2012) Poplar extrafloral nectaries: Two types, two strategies of indirect defenses against herbivores. *Plant Physiol* 159(3):1176–1191.
41. Shabala S, Shabala L (2002) Kinetics of net H4, Ca^{2+}, K$^+$, Na$^+$, NH$_4^+$, and Cl$^-$ fluxes associated with post-chilling recovery of plasma membrane transporters in Zea mays leaf and root tissues. *Physiol Plant* 114(1):47–56.
42. Becker D, et al. (1996) Changes in voltage activation, Cs$^+$ sensitivity, and ion permeability in H5 mutants of the plant K$^+$ channel KAT1. *Proc Natl Acad Sci USA* 93(15):8123–8128.